Intrinsic relationship between photoluminescence and electrical characteristics in modulation Fe-doped AlGaN/GaN HEMTs*

Jianfei Li(李建飞)[1,2], Yuanjie Lv(吕元杰)[2], Changfu Li(李长富)[1], Ziwu Ji(冀子武)[1,†], Zhiyong Pang(庞智勇)[1], Xiangang Xu(徐现刚)[3], and Mingsheng Xu(徐明升)[4]

[1] *School of Microelectronics, Shandong University, Jinan* 250100, *China*
[2] *National Key Laboratory of Application Specific Integrated Circuit (ASIC), Hebei Semiconductor Research Institute, Shijiazhuang* 050051, *China*
[3] *Key Laboratory of Functional Crystal Materials and Device (Ministry of Education), Shandong University, Jinan* 250100, *China*
[4] *School of Physics and Optoelectronics, South China University of Technology, Guangzhou* 510640, *China*

(Received 2 December 2016; revised manuscript received 6 May 2017; published online 18 July 2017)

The photoluminescence (PL) and electrical properties of AlGaN/GaN high electron mobility transistors (HEMTs) with different Fe doping concentrations in the GaN buffer layers were studied. It was found that, at low Fe doping concentrations, the introduction of Fe atoms can result in a downward shift of the Fermi level in the GaN buffer layer, since the Fe atoms substitute Ga and introduce an $Fe_{Ga}^{3+/2+}$ acceptor level. This results in a decrease in the yellow luminescence (YL) emission intensity accompanied by the appearance of an infrared (IR) emission, and a decrease in the off-state buffer leakage current (BLC). However, a further increase in the Fe doping concentration will conversely result in the upward shift of the Fermi level due to the incorporation of O donors under the large flow rate of the Fe source. This results in an increased YL emission intensity accompanied by a decrease in the IR emission intensity, and an increase in the BLC. The intrinsic relationship between the PL and BLC characteristics is expected to provide a simple and effective method to understand the variation of the electrical characteristic in the modulation Fe-doped HEMTs by optical measurements.

Keywords: AlGaN/GaN HEMT, Fe-doping, photoluminescence, leakage current

PACS: 85.30.Tv, 73.40.Kp, 78.55.–m, 73.90.+f **DOI:** 10.1088/1674-1056/26/9/098504

1. Introduction

High electron mobility transistors (HEMTs) based on AlGaN/GaN heterostructures, which contain a polarization-induced high-mobility two-dimensional electron gas (2DEG) at the AlGaN/GaN interfaces, even in the absence of any doping, have been widely studied for their potential application in high-frequency and high-power amplifiers.[1–3] However, AlGaN/GaN heterostructures often show a high buffer leakage current (BLC) due to the high background carrier density in the GaN buffer layer, which may originate from crystalline defects such as vacancies, threading dislocations, and unintentionally incorporated donor impurities such as Si and O.[4,5] Reduction of BLC is extremely important to improve the device performance, and some approaches, such as using C-, Fe-, Cr-, and Mg-doping, have been demonstrated to obtain semi-insulating (SI)-GaN wafers.[6–8] The impurities, as deep acceptors in the form of substitution atoms, can trap electrons, compensating for the donor impurity states in the n-type GaN. Therefore, Fe doping (GaN:Fe) is considered to be one of several promising methods due to its reproducibility and controllability: SI-GaN:Fe substrates and SI-GaN:Fe based transistors have demonstrated high resistivity and high electron mobility, respectively.[9,10] Some articles have discussed the optical or electrical properties of the SI-GaN:Fe bulk films and the SI-GaN:Fe-based HEMTs.[10–14] However, to the best of our knowledge, the investigation of the intrinsic relationship between optical and electrical characteristics in the same SI-GaN:Fe-based HEMT is scarce. Nevertheless, investigating different Fe doping concentrations by optical measurements may be beneficial to understand the variation of the electrical characteristics of the HEMTs due to its simplicity and effectiveness, without the need for full device fabrication.

In this study, three AlGaN/GaN HEMTs with different Fe doping concentrations were grown, and characterised by photoluminescence (PL), Hall-effect, and *I*–*V* measurements. The measurement results showed that the PL and electrical properties of AlGaN/GaN HEMTs depended markedly on the concentration of Fe doping into the GaN buffer layer, and an appropriate Fe doping concentration was necessary to obtain high-performance AlGaN/GaN HEMTs.

2. Experiment

Three types of AlGaN/GaN heterostructures with different Fe doping concentrations were grown on (0001) sapphire substrates using metal–organic chemical vapor deposition (MOCVD). Each AlGaN/GaN heterostructure consisted

*Project supported by the Major Research Plan of the National Natural Science Foundation of China (Grant No. 91433112), the National Natural Science Foundation of China (Grant No. 51672163), and the Key Laboratory of Functional Crystal Materials and Device (Shandong University, Ministry of Education), China (Grant No. JG1401).

†Corresponding author. E-mail: jiziwu@sdu.edu.cn

© 2017 Chinese Physical Society and IOP Publishing Ltd

of a 40-nm-thick low-temperature AlN nucleation layer, followed by a 1.5-μm-thick GaN buffer layer with different Fe doping concentration, a 0.8-μm-thick unintentionally doped GaN buffer layer, a 1-nm-thick AlN interlayer, and a 20-nm-thick AlGaN barrier layer. The Fe doping concentration in the GaN buffer layer was 0 for sample A (i.e., as grown), 1×10^{19} for sample B (slightly-doped), and 2×10^{20} cm^{-3} for sample C (heavily-doped). Figure 1 shows the schematic diagram and optical microscopy image of the AlGaN/GaN HEMT. The HEMT devices with a source–drain spacing of 100 μm and a gate length of 40 μm were fabricated from these AlGaN/GaN heterostructures.

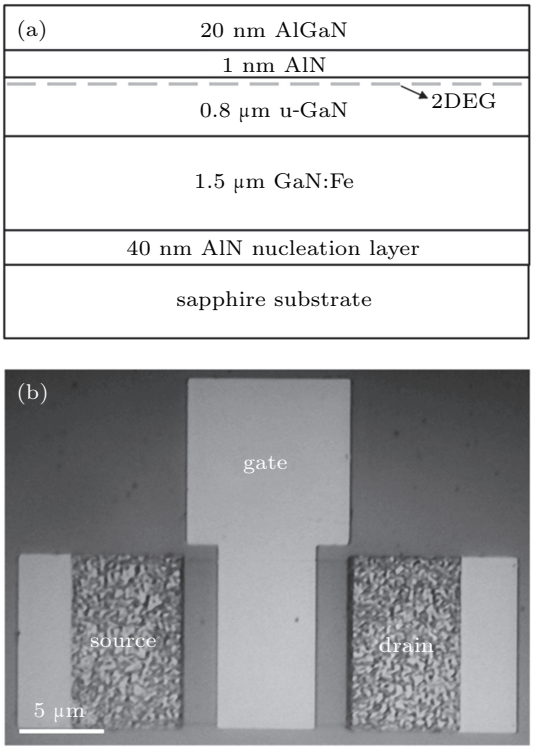


Fig. 1. (a) Schematic diagram and (b) optical microscopy image of AlGaN/GaN HEMT.

The PL spectra were excited using the 325 nm line of a He–Cd laser. The PL signals were analyzed by using a Jobin-Yvon iHR320 monochromator equipped with a thermoelectrically cooled Synapse CCD detector. Hall effect measurements were performed in the van der Pauw geometry on 15 mm square samples, using indium dots as Ohmic contacts. Moreover, *I*–*V* measurements were performed by using an Agilent B1500A semiconductor parameter analyzer.

3. Results and discussion

Figure 2(a) shows the PL spectra of the three samples (samples A–C) measured at 300 K and 0.02 mW. As can be seen in Fig. 2(a), the PL spectrum of the as-grown sample A consists of a near-band edge (NBE) emission at 3.428 eV and a broad band peak at around 2.3 eV. The former originates from the flat-band region of the GaN layer,[15] and the latter is assigned to the transition between the conduction band or shallow donors and the acceptor-type defect complexes composed of Ga vacancies (V_{Ga}) and/or V_{Ga}–O,[10,12,16] this is the so-called yellow luminescence (YL) band. The intensity oscillations of the YL emission are due to Fabry–Perot type interferences. For the doped samples B and C, besides the NBE and YL emissions, a characteristic infrared (IR) emission at 1.287 eV is also observed. In order to establish the origin of the IR emission, we show in Fig. 2(b) the typical temperature-dependent PL spectra in the vicinity of the IR emission peak for sample B as a representative of the doped samples measured in the range 6–300 K. As shown in Fig. 2(b), at 6 K, the PL spectrum is dominated by the zero-phonon line (ZPL) of the internal 3d–3d transition of Fe^{3+}_{Ga} peaking at 1.300 eV with FWHM of 0.825 meV. A set of partially resolved lines in the range 1.21–1.29 eV is identified as the vibrational replica of the ZPL. The additional lines, the so-called "hot lines," in the higher energy side of the ZPL, are attributed to the splitting of the excited $^4T_1(G)$ state of Fe^{3+}_{Ga}.

With increasing temperature below about 230 K, the ZPL intensity gradually decreases, while the intensity of all vibrational replicas increases accompanied by their gradual merging. This behavior can be explained as the gradual increase of the electron–phonon interaction with rising temperature.[13] Above about 230 K, the ZPL component vanishes and the PL spectrum transforms into the 1.287 PL band. Based on this, we conclude that at room temperature, the 1.287 eV IR emission is attributed only to all vibrational replicas of the ZPL. This shows that, in the present study, two nominal Fe-doped structures (i.e., samples B and C) have been successfully grown, and the Fe atoms incorporated in the GaN matrix are substitutional on the Ga site and introduce the charge transfer level ($Fe^{3+/2+}_{Ga}$) in the midgap.

Moreover, it is found from Fig. 2(a) that, among the three samples, the intensity of the YL band is the strongest for sample A and the weakest for sample B.[17] Meanwhile, the intensity of the IR emission of sample C is weaker than that of sample B. Here, it should be noted that all the PL spectra shown in Fig. 2(a) are normalized to the NBE emission. The aforementioned dependence of the PL spectra on the Fe doping concentration shown in Fig. 2(a) can be explained as follows. For sample B, the Fe atoms incorporated in the GaN matrix can substitute Ga and introduce charge transfer level $Fe^{3+/2+}_{Ga}$ in the mid-gap.[10,12] The presence of Fe^{3+}_{Ga} acceptor level-related point defects induces the IR emission, and results in the Fermi level being shifted from the conduction band minimum (CBM) to the mid-gap.[10] Furthermore, the downward shift of the Fermi level in the GaN buffer layer in turn results in the decrease of the V_{Ga} concentration due to the increase of the V_{Ga} formation energy.[10,16] Therefore, compared with

sample A, sample B shows a new IR emission peak and a decreased response at the YL emission intensity.

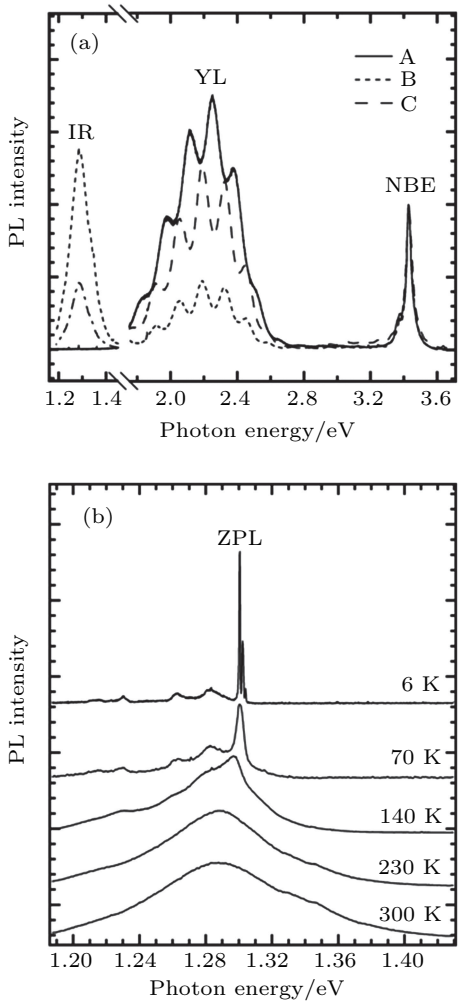


Fig. 2. (a) PL spectra of three AlGaN/GaN HEMTs at $P = 0.02$ mW and $T = 300$ K. All PL spectra are normalized to the near-band edge emission. (b) Temperature-dependent PL spectra in the vicinity of the IR emission peak for sample B.

However, with a further increase in the Fe doping concentration, corresponding to sample C, the density of O donors incorporated into the GaN buffer layer will also increase, since the O contamination is known to originate from the large flow rate of the Fe source (Cp_2Fe).[10,12,18] This results in the increase of the V_{Ga} concentration due to the movement of the Fermi level from the mid-gap to CBM, and the increase of the amount of V_{Ga}–O complexes due to the incorporation of O donors.[10,12] Both lead to the increase of the YL band intensity for sample C compared with that of sample B. Meanwhile, the upward shift of the Fermi level by the O donor incorporation also causes the charge state of the $Fe_{Ga}^{3+/2+}$ level to be transferred from Fe_{Ga}^{3+} to Fe_{Ga}^{2+} by capturing an electron.[10] This process gives rise to the decrease of the Fe_{Ga}^{3+}-related IR emission intensity for sample C compared with that of sample B.

To investigate the influence of the Fe doping concentration on the behavior of 2DEG at the AlGaN/GaN interface, the sheet carrier density and Hall mobility of the three samples as a function of temperature from 10 K to 300 K were measured. As shown in Fig. 3, within the chosen range of measurement, the sheet electron densities of all three samples are practically temperature-independent, and exceed 1.0×10^{13} cm^{-2}. The results indicate an absence of any significant parallel conduction paths and the formation of a 2DEG at the AlGaN/GaN interface in all three samples.[19] In addition, with increasing Fe doping concentration, the sheet electron density first shows only a very slight decrease due to the introduction of the $Fe_{Ga}^{3+/2+}$ acceptor level, and then only a very slight increase perhaps due to the significant incorporation of the O donors (Fig. 3). This indicates that the sheet electron density is barely affected by the Fe doping concentration, and the 2DEG is mainly caused by spontaneous and piezoelectric polarization fields in the AlGaN/GaN heterostructure.

On the other hand, the electron mobility of all the samples first shows a slight decrease below approximately 70 K, and then a significant decrease with further increase in the test temperature (Fig. 3): this is due to the dominance of optical phonon scattering at higher temperatures.[20,21] The measured electron mobilities of the three samples (A, B, and C) are 11690 cm^2/V, 12217 cm^2/V, and 9770 cm^2/V at 10 K, and 1893 cm^2/V, 2031 cm^2/V, and 1532 cm^2/V at room-temperature, respectively. The high electron mobilities of the three samples are consistent with the formation of the 2DEG. In addition, it is found from Fig. 3 that, compared with sample A, samples B and C show a slight increase and an obvious decrease in the electron mobility, respectively, over the whole temperature range tested, particularly in the low temperature range ($T < 200$ K). The former may be due to the decreased electron density in the GaN layer of sample B as mentioned above, the latter may be attributed to the deterioration of the AlGaN/GaN interface quality due to the diffusion of Fe atoms from the Fe-doped GaN buffer layer into the unintentionally doped GaN layer, and even into the AlGaN/GaN interface region of sample C with a larger Fe doping concentration.

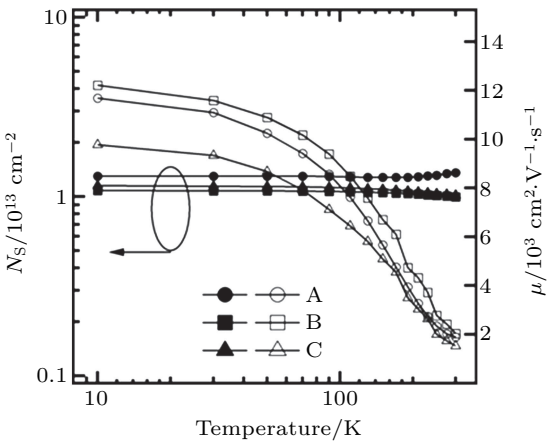


Fig. 3. Temperature dependencies of the sheet carrier density and Hall mobility of the three AlGaN/GaN HEMTs.

To examine the influence of the Fe doping on BLC in AlGaN/GaN HEMTs, the output drain–source currents (I_{DS}) as a function of drain–source voltage (V_{DS}) for the three samples were measured at different gate–source voltages (V_{GS}), and they demonstrated similar trends in their variations. Figure 4(a) shows a typical I_{DS}–V_{DS} characteristic for sample B measured at V_{GS} varying from 0 to −7 V in −0.5 V steps. It is found from Fig. 4(a) that, at $V_{GS} = 0$ V, upon increasing V_{DS} from 0 to 100 V, I_{DS} rapidly increases and reaches a maximum of 2.84 mA at about 5 V, and then decreases upon further increasing V_{DS} due to the negative differential resistance characteristic of self-heating perhaps originating from the poor thermal conductivity of the sapphire substrates.[22–24] Furthermore, when V_{GS} is varied from 0 V, the I_{DS}–V_{DS} curve shifts to a lower value overall, and reaches a minimum at $V_{GS} = -2.5$ V, and then remains almost unchanged up to −7 V. At the same time, in the V_{GS} range from −2.5 V to −7 V, the V_{DS} dependence of I_{DS} also evolves such that, upon increasing V_{DS} from 0 V, I_{DS} first increases slightly ($V_{DS} < 10$ V), and then becomes quasi-saturated upon further increasing V_{DS} to 100 V. The results show that the pinch-off voltage (V_p) of sample B is approximately −2.5 V. In contrast, the V_p for samples A and C are approximately to −3 V.

Figure 4(b) shows the off-state I_{DS} of the three samples as a function of V_{DS} at $V_{GS} = -7$ V. As seen from Fig. 4(b), the off-state I_{DS} measured at $V_{GS} = -7$ V and $V_{DS} = 100$ V is 2.16×10^{-5} for sample A, 1.31×10^{-6} for sample B, and 6.69×10^{-6} A for sample C. The results show that sample B has the lowest off-state I_{DS} compared with samples A and C. The higher off-state I_{DS} for samples A and C means that there is still a non-ignorable conductive channel in the deeper regions of the structure, which is generated by the crystalline defects and donor impurities acting as donor centers.[4,5,22,23]

Based on all the experimental results described above, it may be concluded that, compared with the non-doped sample (such as sample A), a lower Fe doping concentration (1×10^{19} cm^{-3}, such as sample B) can result in a downward shift of the Fermi level in the GaN buffer layer due to the introduction of an $Fe_{Ga}^{3+/2+}$ acceptor level. This leads to a decrease in the YL emission intensity accompanied by the appearance of an IR emission, and a decrease in the BLC. Nevertheless, a higher Fe doping concentration (2×10^{20} cm^{-3}, such as sample C) will conversely result in the upward shift of the Fermi level due to the incorporation of O donors under the large flow rate of the Fe source. This results in an increased YL emission intensity accompanied by a decrease in the IR emission intensity, and an increase in the BLC, compared with the case of the lower Fe doping concentration. To more intuitively display the relationship between the PL and electrical characteristics, we show the quantitative results of the three samples with different Fe doping concentrations in Table 1.

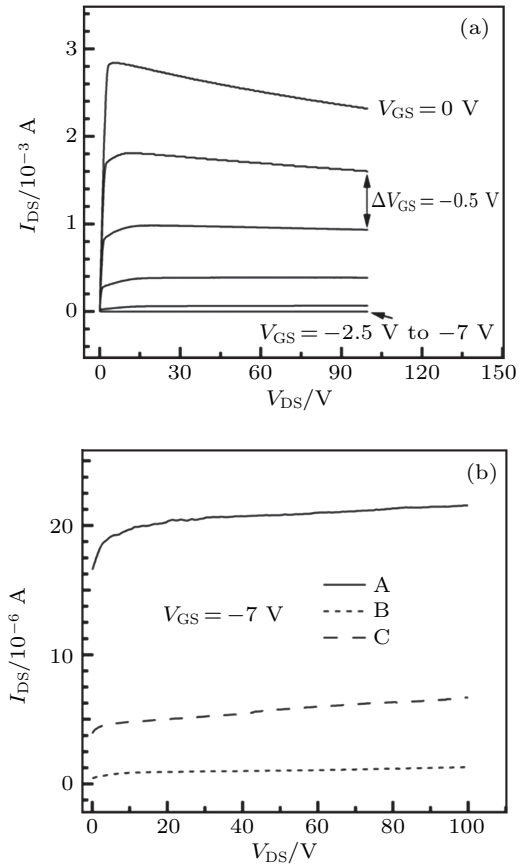


Fig. 4. (a) I_{DS}–V_{DS} curves measured at V_{GS} varying from 0 to −7 V in −0.5 V steps for sample B. (b) Off-state I_{DS} as a function of V_{DS} for the three samples (A, B, and C) at $V_{GS} = -7$ V and $T = 300$ K.

Table 1. Quantitative results of the three samples with different Fe doping concentrations.[a]

Sample	$N_{Fe}/10^{19}$ cm^{-3}	PL		Hall		I–V ($V_{GS} = -7$ V, $V_{DS} = 100$ V)
		I_{YL}/I_{NBE}	I_{IR}/I_{NBE}	$N_S/10^{13}$ cm^{-2}	μ/cm$^2\cdot$V^{-1}	$I_{DS}/10^{-6}$ A
A	0	30.9	0	1.36	1893	21.6
B	1	7.7	18.2	1.00	2031	1.31
C	20	21.0	5.6	1.02	1532	6.69

[a] N_{Fe}, N_S, and μ are the Fe doping concentration, the sheet carrier density, and the Hall mobility, respectively; I_{NBE}, I_{YL}, and I_{IR} are the integrated PL intensity of NBE, YL, and IR emissions, respectively.

Taking into account the above mentioned intrinsic relationship between the PL (YL or/and IR) and BLC characteristics, we find that the study of PL characteristic in AlGaN/GaN HEMTs with different Fe doping GaN buffer layer could be a route to understand the variation of BLC characteristic without the need for full device fabrication. Although more careful experimental investigations are required in future research, the experimental results and the intrinsic relationship between the PL and electrical characteristics obtained in the present work are expected to provide a useful guidance to scientists involved in the fabrication of high-performance AlGaN/GaN HEMTs.

4. Conclusion

The influence of Fe doping concentration on optical and electrical properties in AlGaN/GaN HEMTs was investigated by PL, Hall-effect, and *I*–*V* measurements. The measurement results showed that, compared with the as-grown sample, the slightly doped sample showed a downward shift of the Fermi level in the GaN buffer layer due to the introduction of an $Fe_{Ga}^{3+/2+}$ acceptor level. This resulted in a decrease in the YL emission intensity accompanied by the appearance of an IR emission, and a decrease in the BLC. In contrast, the heavily doped sample showed an upward shift of the Fermi level compared with the slightly doped sample due to the increase of O donors incorporated into the GaN buffer layer under the large flow rate of the Fe source. This resulted in an increased YL emission intensity accompanied by a decrease in the IR emission intensity, and an increase in the BLC, compared with the slightly doped sample. The intrinsic relationship between the PL and BLC characteristics is expected to provide a simple and effective method to understand the variation of the electrical characteristic in the HEMT structure by optical measurements.

References

[1] Marti D, Tirelli S, Alt A R, Roberts J and Bolognesi C R 2012 *IEEE Electron Device Lett.* **33** 1372

[2] He Y L, Wang C, Mi M H, Zheng X F, Zhang M, Zhao M D, Zhang H S, Chen L X, Zhang J C, Ma X H and Hao Y 2016 *Chin. Phys. B* **25** 117305

[3] Wang L, Zhang J Q, Li L, Maeda Y and Ao J P 2017 *Chin. Phys. B* **26** 037201

[4] Moore W J, Freitas Jr J A, Braga G C B, Molnar R J, Lee S K, Lee K Y and Song I J 2001 *Appl. Phys. Lett.* **79** 2570

[5] Ravikiran L, Radhakrishnan K, Munawar Basha S, Dharmarasu N, Agrawal M, Manoj kumar C M, Arulkumaran S and Ng G I 2015 *J. Appl. Phys.* **117** 245305

[6] Hwang C Y, Schurman M J, Mayo W E, Lu Y C, Stall R A and Salagaj T 1997 *J. Electron. Mater.* **26** 243

[7] Monemar B and Lagerstedt O 1979 *J. Appl. Phys.* **50** 6480

[8] Li M, Wang Y, Wong K M and Lau K M 2014 *Chin. Phys. B* **23** 038403

[9] Wu Y F, Saxler A, Moore M, Smith R P, Sheppard S, Chavarkar P M, Wisleder T, Mishra U K and Parikh P 2004 *IEEE Electron Device Lett.* **25** 117

[10] Kubota M, Onuma T, Ishihara Y, Usui A, Uedono A and Chichibu S F 2009 *J. Appl. Phys.* **105** 083542

[11] Desmaris V, Rudziński M, Rorsman N, Hageman P R, Larsen P K, Zirath H, Rödle T C and Jos H F F 2006 *IEEE Tran. Eelectron Dev.* **53** 2413

[12] Dumcenco D O, Levcenco S, Huang Y S, Reynolds Jr C L, Reynolds J G, Tiong K K, Paskova T and Evans K R 2011 *J. Appl. Phys.* **109** 123508

[13] Gladkov P, Hulicius E, Paskova T, Preble E and Evans K R 2012 *Appl. Phys. Lett.* **100** 031908

[14] Axelsson O, Gustafsson S, Hjelmgren H, Rorsman N, Blanck H, Splettstoesser J, Thorpe J, Roedle T and Thorsell M 2016 *IEEE Tran. Eelectron Dev.* **63** 326

[15] Bergman J P, Lundstr?m T, Monemar B, Amano H and Akasaki I 1996 *Appl. Phys. Lett.* **69** 3456

[16] Reshchikov M A and Morkoç H 2005 *J. Appl. Phys.* **97** 061301

[17] Wegscheider M, Simbrunner C, Przybylińska H, Kiecana M, Sawicki M, Navarro-Quezada A, Sitter H, Jantsch W, Dietl T and Bonanni A 2007 *Phys. Status Solidi A* **204** 86

[18] Bonanni A, Kiecana M, Simbrunner C, Li T, Sawicki M, Wegscheider M, Quast M, Przybylińska H, Navarro-Quezada A, Jakieła R, Wolos A, Jantsch W and Dietl T 2007 *Phys. Rev. B* **75** 125210

[19] Smorchkova I P, Chen L, Mates T, Shen L, Heikman S, Moran B, Keller S, DenBaars S P, Speck J S and Mishra U K 2001 *J. Appl. Phys.* **90** 5196

[20] Cao Y and Jena D 2007 *Appl. Phys. Lett.* **90** 182112

[21] Deen D A, Storm D F, Meyer D J, Bass R, Binari S C, Gougousi T and Evans K R 2014 *Appl. Phys. Lett.* **105** 093503

[22] Cordier Y, Azize M, Baron N, Chenot S, Tottereau O and Massies J 2007 *J. Cryst. Growth* **309** 1

[23] Cordier Y, Azize M, Baron N, Bougrioua Z, Chenot S, Tottereau O, Massies J and Gibart P 2008 *J. Cryst. Growth* **310** 948

[24] Lee J, Liu D, Kim H, Schuette M, Flynn J S, Brandes G R and Lu W 2004 *Electron. Lett.* **40** 1227